APPLIED PHYSICS

A nature-inspired ion trap for parallel manipulation of ions on a massive scale

Andrew N. Krutchinsky and Brian T. Chait*

Parallelization has revolutionized computing and DNA sequencing but remains largely unexploited in mass spectrometry (MS), which typically analyzes ions sequentially. Inspired by nuclear cytoplasmic transport, where diffusion governs transport to multiple gated channels (nuclear pore complexes), we introduce an ion trap (MultiQ-IT) that enables massively parallel MS. The device comprises a cubic array of small quadrupoles forming multiple ion entry and exit ports, allowing $>10^9$ ions to be cooled, confined, and manipulated simultaneously. This architecture enables selective depletion of singly charged ions, thereby enhancing signal-to-noise ratios and expanding the effective dynamic range. The trap also functions as a parallel ion splitter, transmitting ions into multiple mass/charge ratio–specific beams. We demonstrate scalable ion throughput, real-time charge discrimination, and parallel beam separation, suggesting a path toward truly parallel MS. Our results establish a conceptual framework for next-generation, high-throughput proteomic and metabolomic analyses.

INTRODUCTION

Mass spectrometry (MS) is now practiced predominantly as a sequential technique, wherein various species in a sample are selected and interrogated one after another (*1*–*3*). Because of the finite time needed to examine each species in turn, such sequential mode MS analysis suffers from inescapable limitations in sensitivity, speed, and the ability to exhaustively analyze all ions produced from the sample, especially when the composition of the ion beam is complex, rapidly changing, highly variable, and of low abundance. The resulting loss of sensitivity makes comprehensive analysis of, e.g., the proteomes of single cells through peptide MS fingerprinting (*4*, *5*) challenging with current approaches. One promising way to address these limitations is through the parallelization of MS analysis, which has the potential to greatly enhance throughput and sensitivity. This concept finds an analogue in parallel computing, where the Gustafson-Barsis law (*6*) has demonstrated the great power of parallelization; but the technology for efficient parallel MS analysis has remained underdeveloped, with a few notable exceptions [e.g., (*7*–*10*)]. In response to this challenge, we have designed and constructed an ion trap architecture (MultiQ-IT) intended for parallel manipulation of ions with the potential for application on a massive scale (*11*–*14*).

RESULTS AND DISCUSSION

The MultiQ-IT was inspired by our research on nucleocytoplasmic transport through nuclear pore complexes (NPCs) and our proposed virtual gating mechanism (*15*, *16*). We envisioned an ion trap analogue of the nucleus, where diffusion serves as the fundamental transport mechanism. However, rather than being embedded with NPCs, this system is engineered with an array of ion input and output ports, enabling ion confinement, controlled transport, and parallel processing. In this design, the ion confinement region is enclosed by a multitude of cylindrical electrodes, systematically arranged around a cube (Fig. 1, A and B, and fig. S1). These electrodes are driven by radio frequency (rf) signals (fig. S2), so that each group of four neighboring cylinders forms a quadrupole. This arrangement of rf quadrupoles, which we term a "MultiQ-Ion Trap (MultiQ-IT)," serves to confine ions within the cubic structure by the ponderomotive forces generated by the rf quadrupole arrays (*17*, *18*). Figure 1C shows an exemplar computed trajectory of a single ion injected into a MultiQ-IT that contains 486 quadrupoles (486Q). The trap operates at a pressure of ~0.1 Pa of nitrogen gas, so that, after injection, ions are rapidly thermalized (usually within a few milliseconds) and begin diffusing inside the ion confinement region. Here, they periodically undergo bouts of reexcitation when ions diffuse into the proximity of the quadrupoles, followed by rethermalization. At the elevated rf amplitude shown, the quadrupoles do not allow passage of the ions through their gaps because the Mathieu stability parameter chosen ($q = 1.28$) lies outside of the $0 < q < 0.9$ stability region (*19*). As we decrease the rf amplitude, ions can occupy a larger volume within the trap and, after thermalization, can defuse between the quadrupoles, whereupon they can escape from the trap along the quadrupole axes (Fig. 1D). Their escape can be prevented either by elevating the potential difference between the quadrupoles and the exterior wall electrodes ($\Delta U = U_{wall} - U_0$) or encouraged by providing specific conditions for ion transport through the quadrupoles and the exterior walls. The conditions for ion transport imposed on each input/output quadrupole port can range from simple, as in a small static potential barrier that prevents thermalized ions from escaping the storage region, to more complex, which may involve operating each quadrupole as a separate filter capable of only transmitting ions with very specific mass/charge ratio (m/z) values (*20*–*22*). To explore the detailed behavior of MultiQ-ITs experimentally, we constructed several versions of the instrument (Fig. 1E) and, over the course of our research, replaced the commercial electrospray sources and interfaces of three different mass spectrometers with our own electrospray interface and MultiQ-IT systems (Fig. 1E). These instruments were used to investigate key properties of the MultiQ-IT, including ion capacity, ion residence time, and the feasibility of using multiple ion trap outputs for the parallel manipulation of ions.

We first conducted a series of experiments that examined mixtures of peptide ions produced by an electrospray ionization source. These ions were introduced into a vacuum interface through a heated

The Rockefeller University, 1230 York Avenue, New York, NY 10065, USA.
*Corresponding author. Email: chait@rockefeller.edu

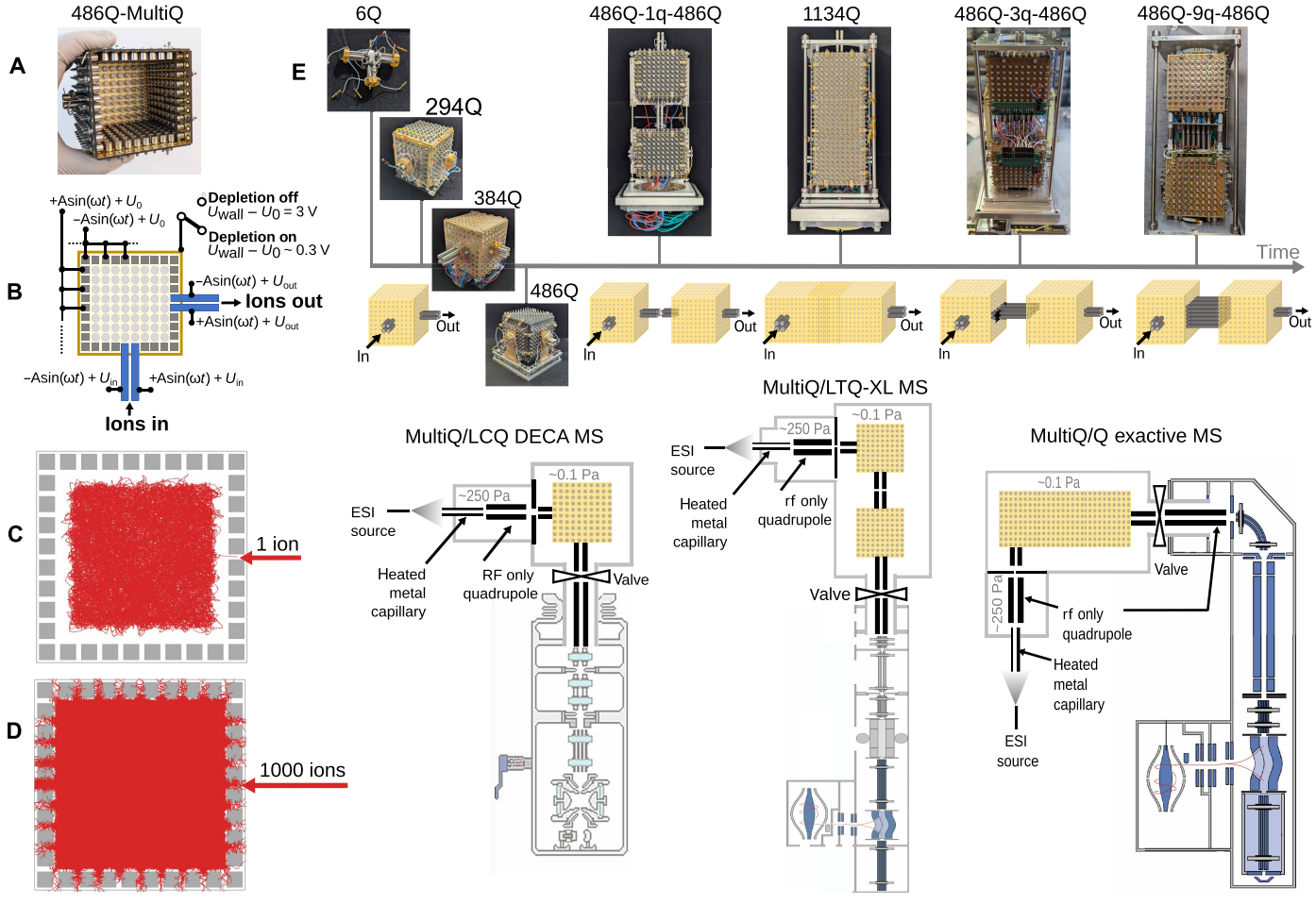

Fig. 1. The MultiQ-IT. (**A**) An optimized 486-quadrupole (486Q) version of a MultiQ-Ion Trap (MultiQ-IT) with one wall removed for clarity. (**B**) Ions are trapped by the radio frequency (rf) fields and a dc potential difference ($\Delta U = U_{wall} - U_0$). (**C**) Simulated trajectory of a single ion (mass of 1500 Da, 3+ charge) projected onto a plane after being trapped with 150 V, 500-kHz rf, and $\Delta U = 4$ V for 1 s. (**D**) Trajectories of 1000 of the same ions as in (C) but with the rf amplitude reduced to 50 V and $\Delta U = 0$. (**E**) Development timeline of MultiQ-IT configurations with increasing numbers of quadrupoles (Q), from 6Q to 1134Q. The 486Q variant was further implemented in tandem configurations (486Q-1q-486Q, 486Q-3q-486Q, and 486Q-9q-486Q), with ion transfer enabled via extended quadrupoles (q). Example implementations into the different mass spectrometers used in the present studies are shown on the bottom right. ESI, electrospray ionization.

metal capillary (*23*, *24*) and directed through an rf-only quadrupole ion guide to a single quadrupole port into the MultiQ-IT. Once trapped, the ions underwent thermalization through collisions with buffer gas molecules (N_2, 0.05 to 0.1 Pa) before exiting through one or more designated ports. The residence half-lives of ions within the trap ranged from 0.1 to 1 s, depending on specific ion characteristics such as molecular weight, charge state, and molecular composition (figs. S3 and S4). Direct ion current measurements demonstrated that the trap can transiently hold as many as 10^9 to 10^{10} elementary charges per second (fig. S5). For ions with charge states ranging from +1 to +6, as determined from the mass spectral data, the maximum measured ion flux through the 486Q ion trap exceeded 10^9 ions/s, which is 1000-fold higher than the capacity of ion traps used in state-of-the-art commercial mass spectrometers (*25*–*27*).

Coulombic repulsion between the large numbers of trapped ions with like charges can generate substantial electric fields, as high as 0.5 to 5 V/mm at the boundary of the ion cloud within the trap (fig. S6). Although the amplitude of the rf trapping signal could theoretically be increased to create a higher effective trapping potential to compensate for this Coulombic repulsion between ions, such an approach is only practical when the ions of interest are not required to explore the space between the quadrupoles. Therefore, to fully use the multiplicity of quadrupole outputs in the trap, the rf amplitude must remain low enough at a given rf frequency to maintain the Mathieu stability parameter of $q < 0.9$; this constraint limits the strength of the effective trapping potential (*28*), in turn limiting the number of ions that can be practically confined in the MultiQ-IT, albeit in the present case to as many as 10^{10} elementary charges.

To evaluate the capability of the MultiQ-IT for manipulating ions in a massively parallel manner, we investigated the ability of the 486Q version to differentiate ions with distinct charge states in real time. Ions attempting to pass through any quadrupole port other than the designated entry and exit ports can be effectively blocked by applying a sufficiently high potential difference between each quadrupole and its nearby wall (Fig. 1B and figs. S1 and S2). Because ions within the trap volume are largely thermalized, a potential difference of just 3 V is sufficient to prevent all ions from exiting. As we reduce the potential difference toward $3/2k_BT$, singly charged ions

begin to overcome the potential barrier, collide with the wall, and are lost. In contrast, thermalized multiply charged ions are less likely to penetrate the barrier, as its effective height increased proportionally with ion charge. Such enrichment of multiply charged ion species was previously observed using a single quadrupole ion trap, where ions (typically with charge states between +1 and +3) were first confined by raising a trapping potential barrier after injection. The barrier was then lowered to selectively deplete singly charged ions, followed by the release and detection of the remaining multiply charged species (*29*, *30*). That approach required a sequential trapping and release mode of operation. In contrast, the MultiQ-IT enables simultaneous operation of a multitude of parallel ports for the selective removal of singly charged ions (in a manner somewhat analogous to online dialysis), greatly improving the efficiency and speed of charge separation. This property was confirmed both computationally (Fig. 2A) and experimentally (Fig. 2B) using several different mass spectrometers equipped with MultiQ-ITs (Fig. 1E). By using the full array of available ports concurrently, singly charged ions were depleted on a timescale comparable to their residence half-life within the trap. This allows real-time charge discrimination as ions transit the trap, eliminating the need for a sequential pulsing sequence.

To determine the number of escape ports required for such efficient real-time depletion, we developed an expanded 1134-quadrupole version of the trap (Fig. 1E). This design, featuring a large number of ports, allowed us to systematically vary the number of exit ports with sufficiently low potential barriers to enable the preferential escape of singly charged ions from a mixed population of ions with charge states ranging from 1+ to 6+ (see, for example, fig. S8, bottom). Our experimental results (Fig. 2C) showed excellent agreement with a theoretical model based on the steady-state solution of Fick's diffusion equation, which describes diffusion toward N circular absorbing apertures in a planar barrier (*31*). The quality of the fit was excellent [$\chi^2 = 0.0011$ and coefficient of determination (R^2) = 0.999999], indicating that ion transport within the MultiQ-IT follows well-established principles of diffusion. For this specific geometry (Fig. 1E), we found that the singly charged ion outflow reaches half of its maximum value when the number of low-potential-barrier exit ports is $N = 39 \pm 3$. This strong alignment between experiment and theory supports our hypothesis that ion motion and escape through multiple ports in the MultiQ-IT can be accurately modeled using the same theoretical framework that describes molecular diffusion to receptors on a cell membrane or transport to NPCs on the periphery of the cell nucleus (*31*).

Next, we investigated whether the depletion process could be further enhanced by coupling two 486-quadrupole ion traps in tandem, each designed to reduce the population of singly charged ions by a factor of ~10 while at the same time efficiently trapping higher-charge-state ions. Because the two traps function independently, their effect in tandem should be multiplicative. As predicted, this approach resulted in a ~100-fold improvement in the signal-to-noise ratio for a low concentration five-peptide test mixture after selectively depleting singly charged ions from the primary ion beam (Fig. 3). Before depletion, peaks corresponding to the peptides were faintly discernable amid a dense background of singly charged ion peaks associated with the so-called chemical noise (Fig. 3A) (*32*). After depletion, however, four of the five peptides in the sample (i.e., those with charge state > 1+) became clearly observable (Fig. 3B). A similar notable effect is seen in Fig. 3 (C and D), where spectra recorded before and after depleting a dominant singly charged contaminant are compared, revealing the previously obscured low intensity protein signal.

Figures S7 to S9 provide additional examples demonstrating the efficacy of the MultiQ-IT in depleting singly charged species across various instrument configurations. In all these cases, we observe great improvements in the signal-to-noise ratios. We also explored the possibility of selectively depleting intermediate charged states (e.g., 2+ and 3+), in addition to 1+, as a strategy to enhance the detection of species with charge states of 4+ or higher (figs. S10 and S11) This approach, which we term "extended charge state depletion," involves appropriately lowering the effective potential barrier to enable the selective escape of 2+ and 3+ ions along with singly charged species. The resulting increase in the relative abundance of higher charge state ions greatly improves the detection of extremely low-level analytes (fig. S12) and holds considerable promise for enhancing the identification of chemically crosslinked species in mass spectrometric workflows (fig. S13) (*33*, *34*), which has become a powerful approach to assist in the integrative structural modeling of large protein-containing assemblies (*35*–*38*). However, to fully unlock the transformative potential of this capability for detecting trace, highly charged species, it will be necessary to implement a truly parallel mass spectrometric system, i.e., one that comprises a large array of dedicated, fragmentation-capable m/z analyzers operating simultaneously, with each channel continuously acquiring data throughout the entire temporal profile of even the weakest signals. Realizing such a system, catalyzed by the development of the MultiQ-IT, represents an ambitious but achievable goal that will require future technical advances.

As an initial step toward this goal, we sought to demonstrate how the MultiQ-IT can support large-scale parallel ion manipulation using its existing architecture. As shown above, applying a modest potential difference across the exits of the MultiQ provides a simple yet effective demonstration of how multiple outputs can be harnessed, without requiring any structural modifications to the original MultiQ-IT design. However, our broader objective is to demonstrate how true massive parallelism in MS can be realized by incorporating more advanced ion transport strategies through these outputs, specifically those capable of real-time beam splitting into multiple, narrow m/z-range subbeams for concurrent detection or analysis. In a first step to explore this concept, we used a tandem MultiQ-IT configuration to evaluate whether multiple output ports could function as independent m/z filters without requiring a separate mass analyzer at each port. In this configuration, the first MultiQ-IT operates as an ion beam splitter, while the second functions as a beam combiner, allowing the output of different channels to be assessed collectively using a single mass analyzer. We began by connecting two traps using three extended quadrupoles and subsequently scaled up to nine, creating systems with three and nine parallel channels, respectively (Fig. 1E). To selectively transmit ions within defined m/z windows, we tested various configurations of the extended quadrupoles, examining their performance as conventional mass filters and as linear traps with axial ion ejection (*20*–*22*, *39*). Unlike prior designs, our approach sought to efficiently return nonresonant ions (those outside a given m/z filter window) back to the interior of the MultiQ-IT, allowing them to further explore and pass through alternative filters better suited to their m/z. Through iterative modeling and prototype testing, we optimized one such design that featured nine extended quadrupoles configured for resonant ion ejection (Fig. 4A). Our modeling included detailed computer simulations of ion motion within a single quadrupole channel (Fig. 4B). These simulations demonstrate efficient and selective ion transmission for target m/z values while

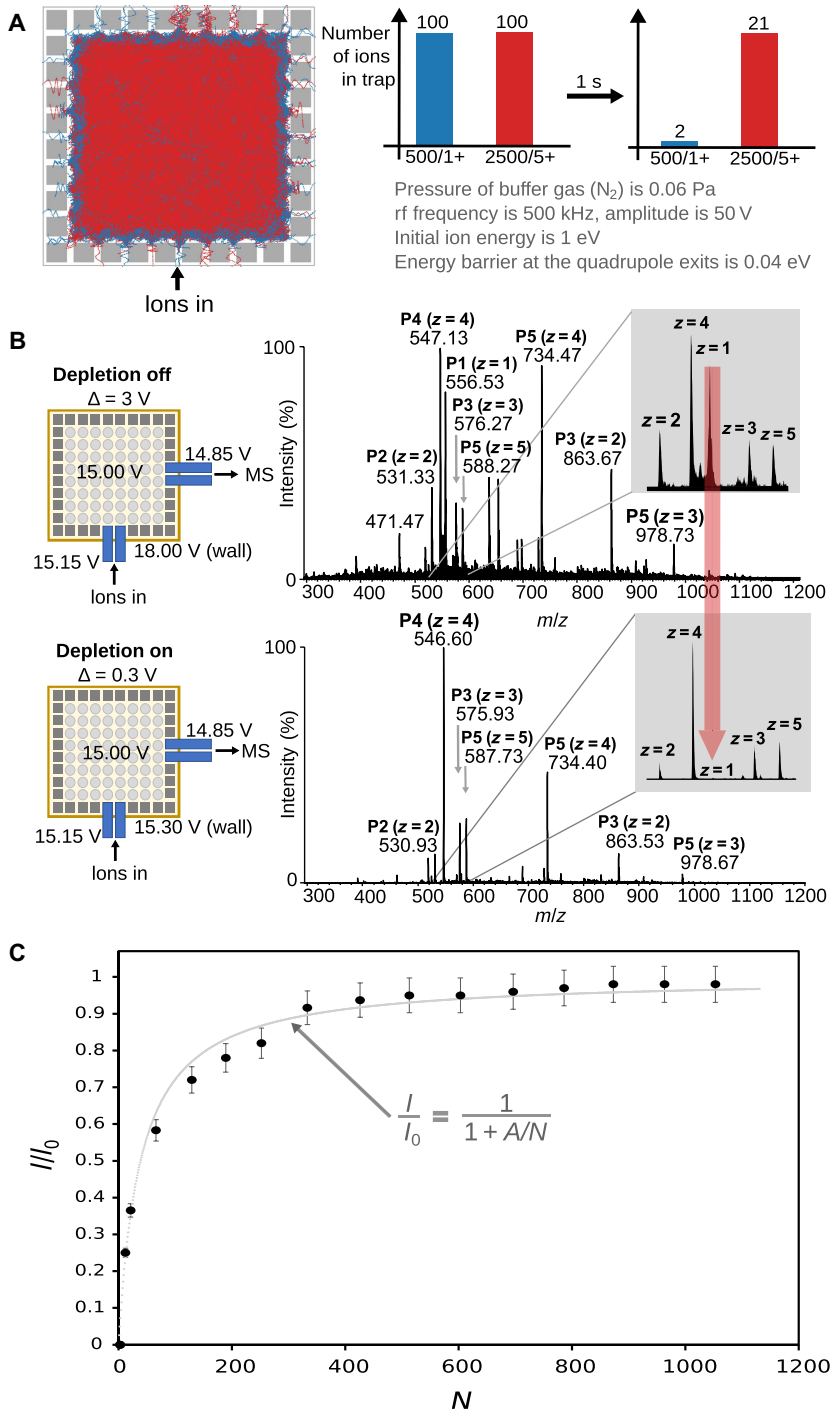

Fig. 2. Selective depletion of singly charged ions using the MultiQ-IT. (**A**) Simulations of 200 ions in the 486Q MultiQ-IT using the Demiurge_MultiQ-IT_486 program (see the Supplementary Materials). Trajectories are shown for 100 singly charged ions ($m/z = 500$; blue) and 100 multiply charged ions ($m/z = 500$, $z = 5$; red), projected onto a plane through the trap midpoint. Ions were tracked for up to 1 s, during which they could remain trapped, exit through a port, or collide with an electrode. (**B**) Experimental validation using a five-peptide mixture (800 amol/s) in a 486Q MultiQ-IT coupled to an LCQ DECA MS. With depletion off (top spectrum), singly charged ions dominate. With depletion on (bottom), singly charged species are reduced, revealing multiply charged peptide signals. Left: Potential distributions used in each mode. Peaks for peptides P1 to P5 are labeled. (**C**) The number of output ports needed for efficient depletion was evaluated by plotting the normalized intensity (I/I_0) of singly charged ions as a function of available ports (N). Increasing N facilitates ion exit, reducing singly charged background in real time.

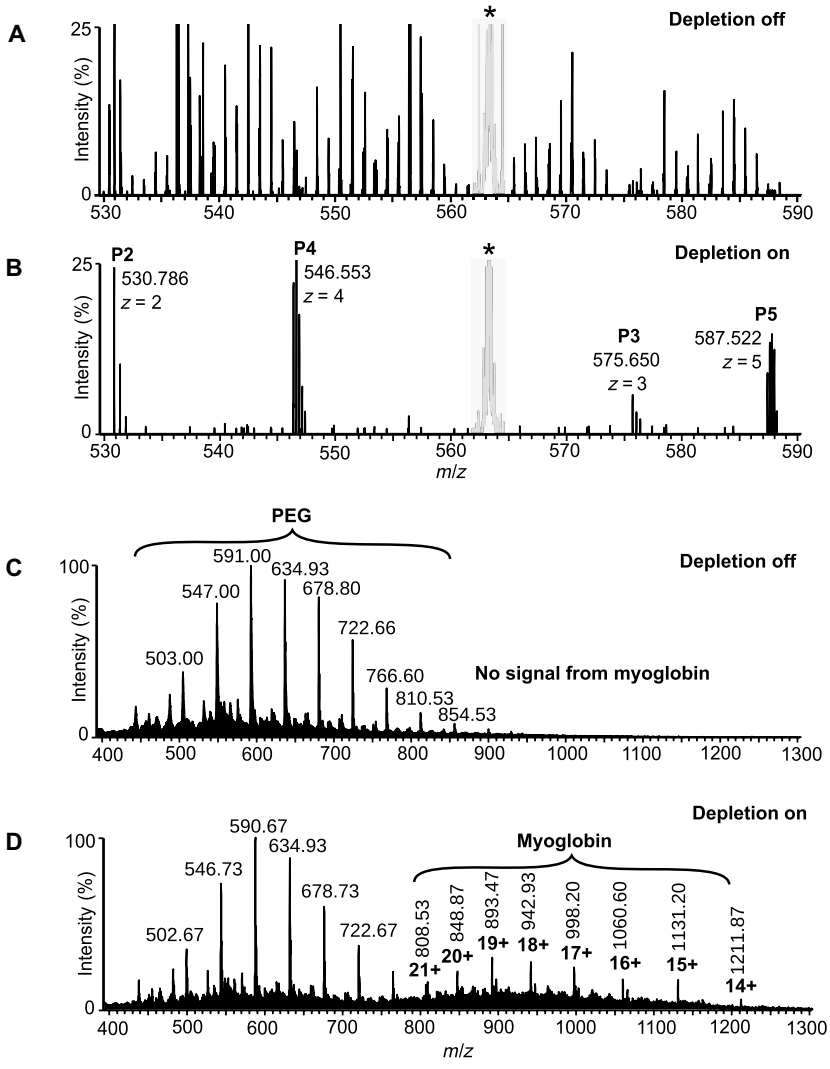

Fig. 3. Signal-to-noise enhancement via selective depletion of singly charged ion background. Portion of the mass spectra arising from a five-peptide mixture electrosprayed at 17 amol/s, recorded without (**A**) and with (**B**) selective depletion of singly charged ions. In the absence of depletion (A), peptide signals are masked by "chemical noise" from abundant singly charged background ions. When depletion mode is enabled (B), using the tandem 486Q MultiQ-IT trap (Fig. 1), singly charged ions are removed in real time as ions transit the trap system. This results in a 100-fold reduction in background, revealing clear signals for four of the five peptides (the singly charged peptide is not observed). Asterisks indicate artifact peaks arising from pickup events in the LTQ-XL mass spectrometer used in this experiment. Mass spectra of myoglobin electrosprayed at 17 amol/s in the presence of a 100-fold molar excess of polyethylene glycol (PEG 500; a common contaminant in protein preparations), recorded without (**C**) and with (**D**) singly charged ion depletion. (C) Depletion off: No signal from myoglobin is observed. (D) Depletion on: Singly charged ions from PEG 500 are preferentially removed, allowing for the observation of the multiply charged myoglobin ion peaks.

maximizing ejection efficiency and minimizing ion losses. The quadrupoles are short (1.2 cm), with two adjacent rods tilted slightly (~0.01 rad) along one axis and parallel along the orthogonal axis, an arrangement that we term the "tilted quadrupole" (Fig. 4A). A small excitation voltage applied across the noninclined rods induces resonant excitation of ions within a specific m/z range, gradually increasing their oscillation amplitude. Once sufficiently displaced, ions encounter the flared potential created by the inclined rods, which accelerate them toward the exit, enabling them to overcome a small stopping potential and leave the MultiQ-IT. Our simulations (Fig. 4C) indicate that this approach should achieve a resolving power of 50 ($\Delta = 10$ at $m/z = 500$), an 80% ejection efficiency at resonance with minimal losses due to collisions with the electrode, and 100% efficiency for return of nonresonant ions to the MultiQ-IT ion confinement region.

Experimental validation of the computationally predicted operation mode of the tandem MultiQ-IT, with two ion traps connected via nine parallel channels (Fig. 1E, top right), is presented in Fig. 5. Ubiquitin ions were selectively transmitted through four of these channels, each tuned to continuously pass ubiquitin ions with a distinct charge state. The system successfully split the incoming ion beam into four distinct subbeams (Fig. 5A), each centered on a selected m/z value and confined within a ±50-m/z unit window. These subbeams were subsequently recombined in the second MultiQ-IT, yielding a composite mass spectrum from all four channels (Fig. 5B). For comparison, Fig. 5C shows the control spectrum obtained by transmitting

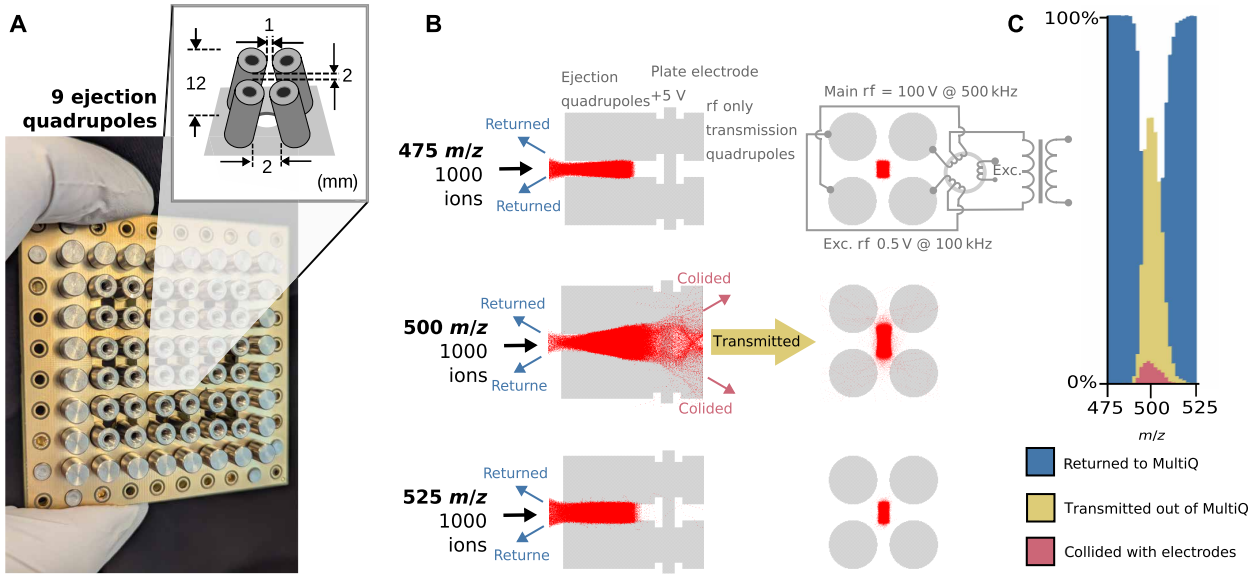

Fig. 4. MultiQ-IT system for continuous ejection of ions into multiple *m/z*-specific subbeams. (**A**) Section of the 486Q MultiQ-IT showing nine tilted ejection quadrupoles integrated into the ion trap wall. The construction and orientation of these quadrupoles enable selective ion transmission. (**B**) Simulations of 1000 ions with *m/z* 475, 500, and 525 entering the tilted quadrupoles. An auxiliary excitation rf is applied to selectively transmit ions centered around *m/z* 500, as indicated. (**C**) Simulation results showing that ions with *m/z* values lower or higher than 500 are returned back into the MultiQ-IT, while ions centered near *m/z* 500 are preferentially transmitted. A minor fraction of partially transmitted ions is lost because of collisions with the quadrupole electrodes.

ubiquitin ions directly from the first to the second trap under a dc gradient, without applying resonant rf excitation, i.e., without *m/z*-selective splitting. In parallel splitting mode, initial ejection efficiency was ~10% of direct transmission, but, with improved rod alignment and optimized ejection parameters, efficiency could be raised to 90 to 100% (fig. S14). Performance losses from charge buildup were alleviated by siphoning excess ions, consistent with the expectation that, as more channels operate in parallel, the ion load per channel decreases and space-charge effects are reduced.

In this work, we have demonstrated that the MultiQ-IT platform holds substantial promise for enabling massively parallel MS, offering a strategy to enhance sensitivity, speed, and dynamic range in MS analyses. Unlike conventional ion traps that operate with a single input and output, requiring sequential ion accumulation and ejection, the MultiQ-IT incorporates multiple quadrupole-based inputs and outputs. These serve two key roles: (i) transient containment and thermalization of ions, as evidenced by our ability to trap and manipulate up to 10^9 ions, exceeding the capacity of existing designs by three orders of magnitude; and (ii) controlled ion release in which ions, through their thermalized random motion, distribute across all available exits, so forming spatially separated subbeams, whose composition can be modulated to optimize downstream analysis.

This ability to generate and manipulate spatially separated ion subbeams is foundational for achieving true massive parallelization in MS. Our findings establish the feasibility of parallel MS using the MultiQ-IT. Much like nucleocytoplasmic transport to and through NPCs, ion movement in the MultiQ-IT is governed by diffusion-driven transport, regulated by the availability and configuration of input and exit ports. In our charge state depletion studies, we found that effective ion depletion requires only a modest number of quadrupole ports, much like NPCs, which efficiently mediate molecular exchange despite their limited number (*40*). Fitting a steady-state solution to Fick's diffusion equation, we determined that a few hundred ports are more than sufficient to achieve optimal ion depletion, mirroring the efficiency of NPCs in biological systems (*31*, *40*). By applying the same diffusion-based framework, we were able to model transport of large macromolecular complexes (here pre-60*S* ribosomal particles) to NPCs in a yeast nucleus of realistic size, NPC number, and experimentally measured diffusion constants (fig. S15) (*40*, *41*). These simulations reinforce the idea that only a limited number of NPCs are sufficient to sustain efficient nucleocytoplasmic transport, suggesting that the principles guiding MultiQ-IT design may also shed light on how biological systems choose NPC numbers and spatial distribution (fig. S16) to balance efficiency and resource cost.

The MultiQ-IT is also highly scalable, following an N^2 relationship [specifically, $6(N-1)^2$ for a cubic configuration, where N represents the number of cylindrical electrodes along a single dimension]. This scalable architecture presents compelling opportunities in proteomics, metabolomics, and single-cell analysis, particularly when each subbeam is coupled with integrated fragmentation and spectrum acquisition capabilities. Recent advances in miniaturized and array-based mass spectrometer systems (*42*) suggest that such capabilities are increasingly within technological reach. The development of the MultiQ-IT is expected to further accelerate these technological advances by providing a robust platform ideally suited for such integration.

The MultiQ-IT represents a substantial advance toward parallel MS, offering avenues to improve speed, sensitivity, dynamic range, redundancy, and system scalability. Just as parallel computing transformed information processing and massively parallel DNA sequencing has revolutionized genomics, the MultiQ-IT may likewise broaden what is possible in analytical science, opening the door to next-generation applications in chemistry, biology, and medicine.

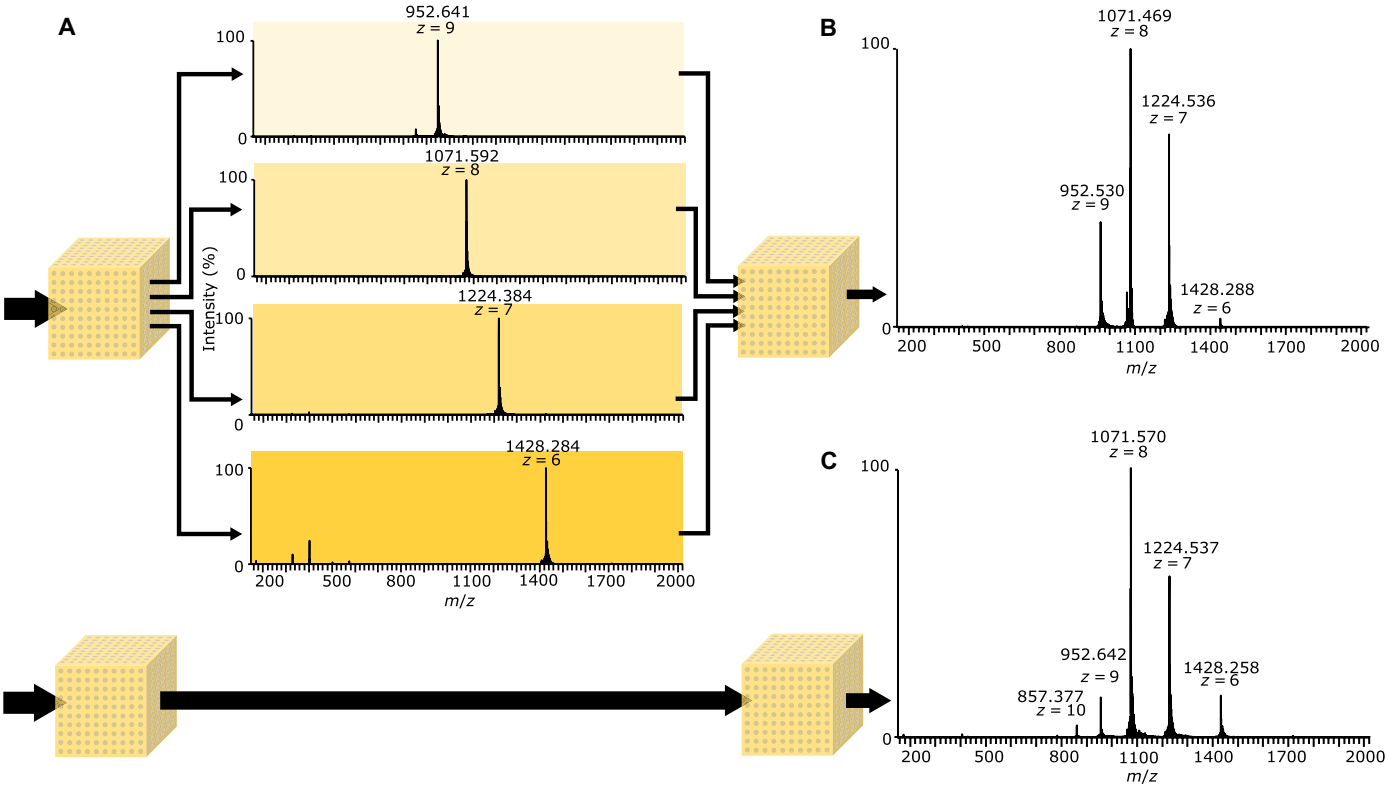

Fig. 5. Splitting an ion beam into parallel subbeams. Four randomly selected channels from the nine available in the tandem MultiQ-IT system were independently optimized to transmit distinct ubiquitin charge states by tuning the resonance frequency (40 to 60 kHz) and rf amplitude (ranging from 1.5 to 5 V) applied to the extended quadrupoles. Once optimized, ion transfer between the first and second MultiQ-IT traps could be selectively blocked by applying a reverse dc gradient. (**A**) *m/z* spectra recorded by selectively activating each channel, allowing isolation and detection of individual charge states. (**B**) Simultaneous activation of all four optimized channels resulted in combined transmission of selected ions into the second MultiQ-IT, generating a composite ubiquitin spectrum. (**C**) Control spectrum acquired by transmitting ubiquitin ions through a single channel without applying any resonant excitation, using only a dc gradient. The observed ion ejection resolution was ~10 (theoretical, ~50). Ubiquitin was chosen for its well-resolved charge states (+6 to +10), making it an ideal model for assessing multichannel selectivity.

MATERIALS AND METHODS

MultiQ-IT instrumentation

Details of the construction and setup of the MultiQ-IT ion trap are shown in figs. S1 and S2. Ion currents were monitored using a low-noise current amplifier (Stanford Research Systems, Model SR570). Pulse generation and resonant excitation of ions were carried out using digital signal generators (Stanford Research Systems, Models DS345 and DG535) and a Koolertron DS Signal Generator/Counter.

Reagents and sample preparation

A mixture of five synthetic peptides (AnaSpec) was prepared at concentrations ranging from 1 to 100 fmol/μl in 0.01% formic acid in 70:30 (v/v) water/acetonitrile. The peptide mixture included the following: [Leu^5]-Enkephalin (YGGFL, 555.269 Da; AS-24333); [Des-Pro^2]–Bradykinin (RPPGFSPFR, 1059.561 Da; AS-20667); Bak BH3 (GQVGRQLAIIGDDINR, 1723.933 Da; AS-61616); Neuropeptide S, mouse (SFRNGVGSGAKKTSFRRAKQ, 2181.188 Da; AS-61246); and ACTH (1–24), human (SYSMEHFRWGKPVGKKRRPVKVYP, 2931.580 Da; AS-20613).

This mixture generated distinct ESI peaks in the 500- to 600-*m/z* range, with ion charge states from +1 to +5, enabling detailed evaluation of depletion and trapping performance. Other analytes used included ubiquitin (bovine erythrocytes; Sigma-Aldrich, U6253), myoglobin (equine heart; Sigma-Aldrich, M1882), and polyethylene glycol (PEG 350; Fluka, 81318), prepared at 0.1 to 1 pmol/μl in the same solvent.

Software and data analysis

Mass spectra were visualized using Xcalibur and FreeStyle (Thermo Fisher Scientific). Spectra are presented unprocessed unless otherwise noted. Ion motion within the MultiQ-IT was simulated using custom processing and Java-based software on the basis of a previously described model (*43*). This simulation code is available via https://github.com/akrutchins and is permanently archived in Zenodo (https://doi.org/10.5281/zenodo.17770825, https://doi.org/10.5281/zenodo.17770819, https://doi.org/10.5281/zenodo.17770795, and https://doi.org/10.5281/zenodo.18611066).

Supplementary Materials

This PDF file includes:

Figs. S1 to S16

REFERENCES

1. Y. Y. Zhang, B. R. Fonslow, B. Shan, M.-C. Baek, J. R. Yates III, Protein analysis by shotgun/bottom-up proteomics. *Chem. Rev.* **113**, 2343–2394 (2013).
2. R. Aebersold, M. Mann, Mass-spectrometric exploration of proteome structure and function. *Nature* **537**, 347–355 (2016).

3. H. I. Stewart, D. Grinfeld, A. Giannakopulos, J. Petzoldt, T. Shanley, M. Garland, E. Denisov, A. C. Peterson, E. Damoc, M. Zeller, T. N. Arrey, A. Pashkova, S. Renuse, A. Hakimi, A. Kühn, M. Biel, A. Kreutzmann, B. Hagedorn, I. Colonius, A. Schütz, A. Stefes, A. Dwivedi, D. Mourad, M. Hoek, B. Reitemeier, P. Cochems, A. Kholomeev, R. Ostermann, G. Quiring, M. Ochmann, S. Möhring, A. Wagner, A. Petker, S. Kanngiesser, M. Wiedemeyer, W. Balschun, D. Hermanson, V. Zabrouskov, A. A. Makarov, C. Hock, Parallelized acquisition of orbitrap and astral analyzers enables high-throughput quantitative analysis. *Anal. Chem.* **95**, 15656–15664 (2023).
4. A.-D. Brunner, M. Thielert, C. Vasilopoulou, C. Ammar, F. Coscia, A. Mund, O. B. Hoerning, N. Bache, A. Apalategui, M. Lubeck, S. Richter, D. S. Fischer, O. Raether, M. A. Park, F. Meier, F. J. Theis, M. Mann, Ultra-high sensitivity mass spectrometry quantifies single-cell proteome changes upon perturbation. *Mol. Syst. Biol.* **18**, e10798 (2022).
5. R. G. Huffman, A. Leduc, C. Wichmann, M. Di Gioia, F. Borriello, H. Specht, J. Derks, S. Khan, L. Khoury, E. Emmott, A. A. Petelski, D. H. Perlman, J. Cox, I. Zanoni, N. Slavov, Prioritized mass spectrometry increases the depth, sensitivity and data completeness of single-cell proteomics. *Nat. Methods* **20**, 714–722 (2023).
6. J. L. Gustafson, Reevaluating Amdahl's law. *Commun. ACM* **31**, 532–533 (1988).
7. S. G. Park, G. A. Anderson, J. E. Bruce, Parallel spectral acquisition with orthogonal ICR cells. *J. Am. Soc. Mass Spectrom.* **28**, 515–524 (2017).
8. A. A. Makarov, S. Horning, S. R. Horning, Parallel mass analysis. US Patent 7,985,950 B2 (2011).
9. E. R. Badman, R. G. Cooks, A parallel miniature cylindrical ion trap array. *Anal. Chem.* **72**, 3291–3297 (2000).
10. E. R. Badman, R. G. Cooks, Cylindrical ion trap array with mass selection by variation in trap dimensions. *Anal. Chem.* **72**, 5079–5086 (2000).
11. A. N. Krutchinsky, V. Sherman, H. Cohen, B. T. Chait, Multi-pole ion trap for mass spectrometry-1. US Patent 8,637,817 B1 (2014).
12. A. N. Krutchinsky, V. Sherman, H. Cohen, B. T. Chait, Multi-pole ion trap for mass spectrometry-2. US Patent 8,866,076 B2 (2014).
13. A. N. Krutchinsky, V. Sherman, H. Cohen, B. T. Chait, Multi-pole ion trap for mass spectrometry-3. US Patent 9,129,789 B2 (2015).
14. A. N. Krutchinsky, V. Sherman, H. Cohen, B. T. Chait, Multi-pole ion trap for mass spectrometry-4. US Patent 9,299,550 B2 (2016).
15. M. P. Rout, J. D. Aitchison, A. Suprapto, K. Hjertaas, Y. M. Zhao, B. T. Chait, The yeast nuclear pore complex: Composition, architecture, and transport mechanism. *J. Cell Biol.* **148**, 635–651 (2000).
16. M. P. Rout, J. D. Aitchison, M. O. Magnasco, B. T. Chait, Virtual gating and nuclear transport: The hole picture. *Trends Cell Biol.* **13**, 622–628 (2003).
17. J. Franzen, M. Schubert, Method and device for the reflection of charged particles on surfaces. US Patent 5,572,035 A (1996).
18. C. M. Whitehouse, D. G. Welkie, L. Cousins, RF surfaces and RF ion guides. US Patent 7,365,317 B2 (2008).
19. R. E. March, J. F. J. Todd, *Practical Aspects of Ion Trap Mass Spectrometry Volume 1: Fundamentals of Ion Trap Mass Spectrometry*, T. Cairns, Ed., CRC Series Modern Mass Spectrometry (CRC Press, 1995).
20. A. E. Holme, Operation of a quadrupole mass filter with only an R.F. voltage component applied to the rod system. *Int. J. Mass Spectrom. Ion Processes* **22**, 1–5 (1976).
21. U. Brinkmann, A modified quadrupole mass filter for the separation of ions of higher masses with high transmission. *Int. J. Mass Spectrom. Ion Phys.* **9**, 161–166 (1972).
22. F. A. Londry, J. W. Hager, Mass selective axial ion ejection from a linear quadrupole ion trap. *J. Am. Soc. Mass Spectrom.* **14**, 1130–1147 (2003).
23. S. K. Chowdhury, V. Katta, B. T. Chait, An electrospray ionization mass spectrometer with new features. *Rapid Commun. Mass Spectrom.* **4**, 81–87 (1990).
24. S. K. Chowdhury, V. Katta, B. T. Chait, Electrospray ionization mass spectrometer with new features. US Patent 4,977,320 (1990).
25. C. M. Rose, J. D. Russell, A. R. Ledvina, G. C. McAlister, M. S. Westphall, J. Griep-Raming, J. C. Schwartz, J. J. Coon, J. E. P. Syka, Multipurpose dissociation cell for enhanced ETD of intact protein species. *J. Am. Soc. Mass Spectrom.* **24**, 816–827 (2013).
26. N. M. Riley, C. Mullen, C. R. Weisbrod, S. Sharma, M. W. Senko, V. Zabrouskov, M. S. Westphall, J. E. P. Syka, J. J. Coon, Enhanced dissociation of intact proteins with high capacity electron transfer dissociation. *J. Am. Soc. Mass Spectrom.* **27**, 520–531 (2016).
27. R. A. Zubarev, A. Makarov, Orbitrap mass spectrometry. *Anal. Chem.* **85**, 5288–5296 (2013).
28. D. Gerlich, Inhomogenous RF-fields - A versatile tool for the study of processes with slow ions. *Adv. Chem. Phys.* **82**, 1–176 (1992).
29. J. W. Hager, Method of mass spectrometry, to enhance seperation of ions with different charges. US Patent 2,004,183,005 A1 (2004).
30. A. V. Tolmachev, A. N. Vilkov, L. Pasa-Tolic, H. R. Udseth, R. D. Smith, Suppression of the lower charge state ions in the external accumulation RF multipole with a reduced trapping DC potential. *J. Am. Soc. Mass Spectrom.* **14**, 1229–1235 (2003).
31. H. C. Berg, *Random Walks in Biology: New and Expanded Edition* (Princeton Univ. Press, 1983).
32. A. N. Krutchinsky, B. T. Chait, On the nature of the chemical noise in MALDI mass spectra. *J. Am. Soc. Mass Spectrom.* **13**, 129–134 (2002).
33. A. Maiolica, D. Cittaro, D. Borsotti, L. Sennels, C. Ciferri, C. Tarricone, A. Musacchio, J. Rappsilber, Structural analysis of multiprotein complexes by cross-linking, mass spectrometry, and database searching. *Mol. Cell. Proteomics* **6**, 2200–2211 (2007).
34. A. Leitner, T. Walzthoeni, A. Kahraman, F. Herzog, O. Rinner, M. Beck, R. Aebersold, Probing native protein structures by chemical cross-linking, mass spectrometry, and bioinformatics. *Mol. Cell. Proteomics* **9**, 1634–1649 (2010).
35. C. W. Akey, D. Singh, C. Ouch, I. Echeverria, I. Nudelman, J. M. Varberg, Z. L. Yu, F. Fang, Y. Shi, J. J. Wang, D. Salzberg, K. K. Song, C. Xu, J. C. Gumbart, S. Suslov, J. Unruh, S. L. Jaspersen, B. T. Chait, A. Sali, J. Fernandez-Martinez, S. J. Ludtke, E. Villa, M. P. Rout, Comprehensive structure and functional adaptations of the yeast nuclear pore complex. *Cell* **185**, 361–378 (2022).
36. F. Alber, S. Dokudovskaya, L. M. Veenhoff, W. H. Zhang, J. Kipper, D. Devos, A. Suprapto, O. Karni-Schmidt, R. Williams, B. T. Chait, A. Sali, M. P. Rout, The molecular architecture of the nuclear pore complex. *Nature* **450**, 695–701 (2007).
37. F. Alber, S. Dokudovskaya, L. M. Veenhoff, W. Z. Zhang, J. Kipper, D. Devos, A. Suprapto, O. Karni-Schmidt, R. Williams, B. T. Chait, M. P. Rout, A. Sali, Determining the architectures of macromolecular assemblies. *Nature* **450**, 683–694 (2007).
38. S. J. Kim, J. Fernandez-Martinez, I. Nudelman, Y. Shi, W. Z. Zhang, B. Raveh, T. Herricks, B. D. Slaughter, J. A. Hogan, P. Upla, I. E. Chemmama, R. Pellarin, I. Echeverria, M. Shivaraju, A. S. Chaudhury, J. J. Wang, R. Williams, J. R. Unruh, C. H. Greenberg, E. Y. Jacobs, Z. H. Yu, M. J. de la Cruz, R. Mironska, D. L. Stokes, J. D. Aitchison, M. F. Jarrold, J. L. Gerton, S. J. Ludtke, C. W. Akey, B. T. Chait, A. Sali, M. P. Rout, Integrative structure and functional anatomy of a nuclear pore complex. *Nature* **555**, 475–482 (2018).
39. X. Zhang, Y. Wang, L. Hu, D. Guo, X. Fang, M. Zhou, W. Xu, Reducing space charge effects in a linear ion trap by rhombic ion excitation and ejection. *J. Am. Soc. Mass Spectrom.* **27**, 1256–1262 (2016).
40. M. Winey, D. Yarar, T. H. Giddings Jr., D. N. Mastronarde, Nuclear pore complex number and distribution throughout the *Saccharomyces cerevisiae* cell cycle by three-dimensional reconstruction from electron micrographs of nuclear envelopes. *Mol. Biol. Cell* **8**, 2119–2132 (1997).
41. J. A. Ruland, A. M. Krüger, K. Dörner, R. Bhatia, S. Wirths, D. Poetes, U. Kutay, J. P. Siebrasse, U. Kubitscheck, Nuclear export of the pre-60S ribosomal subunit through single nuclear pores observed in real time. *Nat. Commun.* **12**, 6211 (2021).
42. P. Mielczarek, J. Silberring, M. Smoluch, Miniturization in mass spectrometry. *Mass Spectrom. Rev.* **39**, 453–470 (2020).
43. A. N. Krutchinsky, I. V. Chernushevich, V. L. Spicer, W. Ens, K. G. Standing, Collisional damping interface for an electrospray ionization time-of-flight mass spectrometer. *J. Am. Soc. Mass Spectrom.* **9**, 569–579 (1998).

Acknowledgments: We would like to thank H. Cohen for assistance with electronics during the early stages of this work. We also thank S. Kent and M. Rout for reading the draft manuscript and providing us with feedback and encouragement. **Funding:** This work was supported by a NIH Director's Transformative Research Award to BTC (PHS R01GM136654) and in the early stages by the Robertson Therapeutic Development Fund and by unrestricted funds from The Rockefeller University. **Author contributions:** Conceptualization: A.N.K. and B.T.C. Methodology: A.N.K. and B.T.C. Software: A.N.K. Validation: A.N.K. and B.T.C. Formal analysis: A.N.K. and B.T.C. Investigation: A.N.K. and B.T.C. Resources: A.N.K. and B.T.C. Data curation: A.N.K. and B.T.C. Writing—original draft: A.N.K. and B.T.C. Writing—review and editing: A.N.K. and B.T.C. Visualization: A.N.K. and B.T.C. Supervision: B.T.C. Project administration: A.N.K. and B.T.C. Funding acquisition: B.T.C. **Competing interests:** A.N.K. and B.T.C. are inventors on patents related to the MultiQ-IT technology owned by The Rockefeller University (US patent nos. 8,637,817 B1; 8,866,076 B2; 9,129,789 B2; and 9,299,550 B2). The other authors declare that they have no competing interests. **Data, code, and materials availability:** All data and code needed to evaluate and reproduce the results in the paper are present in the paper and/or the Supplementary Materials. The authors declare no new materials were generated in this paper. Simulation code is available via https://github.com/akrutchins and is permanently archived in Zenodo (https://doi.org/10.5281/zenodo.17770825, https://doi.org/10.5281/zenodo.17770819, https://doi.org/10.5281/zenodo.17770795, and https://doi.org/10.5281/zenodo.18611066).

Submitted 29 September 2025
Accepted 13 February 2026
Published 18 March 2026
10.1126/sciadv.aec7048

Science Advances

A nature-inspired ion trap for parallel manipulation of ions on a massive scale

Andrew N. Krutchinsky and Brian T. Chait

Sci. Adv. **12** (12), eaec7048. DOI: 10.1126/sciadv.aec7048

Science Advances (ISSN 2375-2548) is published by the American Association for the Advancement of Science. 1200 New York Avenue NW, Washington, DC 20005. The title *Science Advances* is a registered trademark of AAAS.